The Effect of Vertical Baroclinicity Concentration on Atmospheric Macroturbulence Scaling Relations

JANNI YUVAL AND YOHAI KASPI

Department of Earth and Planetary Sciences, Weizmann Institute of Science, Rehovot, Israel

(Manuscript received 28 September 2016, in final form 29 January 2017)

ABSTRACT

Motivated by the expectation that under global warming upper-level meridional temperature gradients will increase while lower-level temperature gradients will decrease, the relations between the vertical structure of baroclinicity and eddy fields are investigated. The sensitivity of eddies and the relation between the mean available potential energy and eddy quantities are studied for cases where the vertical structure of the lapse rate and meridional temperature gradient are modified. To investigate this systematically, an idealized general circulation model with a Newtonian cooling scheme that has a very short relaxation time for the mean state and a long relaxation time for eddies is used. This scheme allows for any chosen zonally mean state to be obtained with good precision. The results indicate that for similar change in the lapse rate or meridional temperature gradient, eddies are more sensitive to changes in baroclinicity where it is already large. Furthermore, when the vertical structure of the lapse rate or the meridional temperature gradient is modified, there is no universal linear relation between the mean available potential energy and eddy quantities.

1. Introduction

Relating eddy fields to the mean state has been a fundamental problem in geophysical fluid dynamics. Charney (1947) and Eady (1949) related the linear growth rate of disturbances to the mean state, and the Eady growth rate is used extensively in climate dynamics and can often assist in understanding the response of the eddies to changes in the mean state (e.g., Hoskins and Valdes 1990; Li and Battisti 2008; Merlis and Schneider 2009). Various closure schemes have been suggested to relate eddy fluxes to the mean state (e.g., Green 1970; Stone 1972; Held 1978). Most closure schemes rely on qualitative arguments that neglect some of the physical details, and therefore their use is limited in cases where these details play an important role. For example, when the vertical structure of baroclinicity is not uniform, their prediction is very limited (e.g., Held and O'Brien 1992; Pavan 1996; Yuval and Kaspi 2016). Schneider and Walker (2008) and O'Gorman and Schneider (2008) showed that for a wide range of parameters, idealized GCM simulations follow semiempirical scaling laws relating linearly the eddy kinetic energy (EKE) to the mean available potential energy (MAPE) derived by Lorenz (1955). Furthermore, Schneider and Walker (2008) obtained a semiempirical scaling between vertically averaged eddy momentum flux (EMF) convergence and surface eddy heat flux (EHF) to MAPE. Schneider and Walker (2008) used a macroturbulence closure that linearly relates eddy available potential energy (EAPE) to MAPE and showed that this closure is consistent with a linear relation between EKE and eddy fluxes to MAPE. Later, O'Gorman (2010) showed that the linear scaling between EKE and MAPE approximately holds for reanalysis data as well as in global warming simulations. O'Gorman (2010) used the MAPE changes in global warming simulations to explain the variability in the EKE between different models. The fact that MAPE and EKE scale linearly also on Earth (O'Gorman 2010), where there are zonal asymmetries and time-dependent diabatic heating, implies that the scaling is robust and is not limited to idealized models.

One of the most robust trends of global warming modeling experiments is that the equator-to-pole temperature difference in the upper levels of the

Corresponding author e-mail: Janni Yuval, yaniyuval@gmail.com

DOI: 10.1175/JAS-D-16-0277.1

atmosphere increases, while in the lower levels there is an opposite tendency (e.g., Manabe and Wetherald 1975; Vallis et al. 2015), especially in Northern Hemisphere winter (Wu et al. 2012). Consequently, the baroclinicity tends to strengthen in the upper troposphere but weaken in the lower troposphere. Therefore, the question of whether knowledge about the temperature distribution of the mean state is sufficient for predicting the eddy response also when the vertical structure of baroclinicity changes is very important in the context of global warming.

Held and O'Brien (1992) used a three-layer quasi-geostrophic (QG) model to study how eddies respond to changes in the vertical structure of wind shear (or temperature gradient). They concluded that for equal values of mean vertical shear, the eddy fluxes are greater when the shear is concentrated at the lower levels ($U_{zz} < 0$). Later, Pavan (1996) showed similar results in a multilayer QG model. Differently, in Yuval and Kaspi (2016) we showed in an idealized GCM that eddies are more sensitive to the upper-level baroclinicity. We hypothesized that eddies are sensitive to large concentration of shear, and since the baroclinicity was larger in the upper levels, eddies were more sensitive to the baroclinicity changes at these levels. This hypothesis is consistent with the idea that EKE, EMF, and EHF are linearly related to MAPE; since MAPE is a nonlinear function of the meridional temperature gradient and lapse rate [MAPE $\propto (\partial_y T)^2/\partial_z T$; Schneider and Walker 2008], changes in the temperature gradient or lapse rate by a certain amount lead to a larger change in MAPE if the changes occur in regions of large local baroclinicity (see definition below). Consequently, the changes in the eddy fields are larger. In Yuval and Kaspi (2016) we showed in an Eady-like model with stepwise shear that the maximal growth rate is mainly sensitive to concentration of shear and less to the mean shear. Namely, the maximal growth rate is sensitive to changes in baroclinicity in regions where it is predominantly large. See appendix A for a detailed explanation of how the results of Held and O'Brien (1992) and Yuval and Kaspi (2016) are consistent.

In this paper, the validity of the linear scaling of EKE and eddy fluxes with MAPE and the response of eddies to changes in the vertical structure of the lapse rate and the meridional temperature gradient are investigated. In addition, to further investigate how a meridional temperature gradient concentration affects eddies and the relation between EKE, eddy fluxes, and MAPE, the meridional temperature gradient was systematically modified at different latitudinal regions in the baroclinic zone. This allows the meridional temperature gradient to be modified, while keeping the lapse rate constant and the vertical structure unchanged, testing the sensitivity of eddies to changes in the meridional gradient alone in regions where baroclinicity is large. This paper broadens the results of Yuval and Kaspi (2016) that studied the sensitivity of eddies to changes in the vertical structure of baroclinicity as a result of changes in the meridional temperature gradient but did not study the response of eddies to changes in the lapse rate or meridional structure changes in the meridional temperature gradient.

Since MAPE is not a local quantity (Lorenz 1955), and the temperature modifications in the simulations in this paper are local, a local measure of instability is needed in order to discuss how the structure of the temperature field affects eddies. As in other studies, the Eady growth rate is used as a local baroclinic instability measure to evaluate changes in baroclinicity of the mean state (e.g., Hoskins and Valdes 1990; Lorenz and Hartmann 2001; Wu et al. 2011). The use of the Eady growth rate as a baroclinicity measure assists in discussing qualitative changes in the simulations, and it is not expected that a local large Eady growth rate would necessarily mean a large local EKE. The use of the Eady growth rate is problematic because (i) it is a linear growth rate of an idealized one-dimensional problem with no horizontal spatial dependence, and the real growth rate might differ from the Eady growth rate; (ii) in the simulations we calculate the saturated EKE and not the growth rate, and there is no a priory reason that the linear growth rate is necessarily correlated with the saturated EKE that depends on nonlinear processes. Despite these limitations we find the Eady growth rate as a useful local measure of instability. Other measures of instability such as supercriticality (Held and Larichev 1996), which are also a function of the meridional temperature gradient divided by static stability ($\propto \partial_y T/N$, where N is the Brunt–Väisälä frequency), will not make a qualitative difference since the Eady growth rate has similar dependence on the meridional temperature gradient and static stability.

The paper is organized as follows. In section 2 the idealized GCM (section 2a) and the method to control the temperature field (section 2b) are described. In section 3 the different temperature profile variations used in the simulations are presented. In section 4 the results of the simulations are presented, particularly focusing on the relation between EKE, EHF, EMF, and changes in the mean temperature profile and MAPE. In section 5 the results are discussed and summarized.

2. Methods

a. Idealized GCM model description

A dry version of an idealized GCM based on the spectral dynamical core of the Geophysical Fluid Dynamics Laboratory (GFDL) Flexible Modeling System (FMS) is used. The model is driven by a Newtonian cooling scheme that is described in section 2b. The simulations do not include orography or ocean, and dissipation in the boundary layer is represented by linear damping of near surface winds (below $\sigma = 0.7$) with a relaxation time of 1 day at the surface [see Held and Suarez (1994) for details]. All simulations have 60 vertical sigma levels with a T42 ($2.8° \times 2.8°$) horizontal resolution. What distinguishes our simulations from Held and Suarez (1994) is the relaxation temperatures and the relaxation time used in the simulations. These are discussed in sections 2b and 3.

All simulations are integrated over 2000 days, where the first 500 days of each simulation are treated as spinup, and the results are averaged over the last 1500 days. All the simulations are hemispherically symmetric and results are presented after averaging over both hemispheres.

b. Forcing the mean state

To methodically change the vertical structure of the lapse rate and meridional temperature gradient, a heating formulation that was suggested by Zurita-Gotor (2007) is used. The main difference of this method to other heating formulations used in idealized models is the usage of different relaxation time scales for the eddies and the zonal mean. The temperature equation in this formulation can be written as

$$\partial_t T = \cdots - \alpha_T (T - \overline{T}) - \alpha_T \gamma (\overline{T} - T_R), \qquad (1)$$

where $\overline{T}$ is the zonal and time mean of field T; α_T is the relaxation time of eddies, and is chosen to be as in Held and Suarez (1994); $\alpha_T \gamma$ is the relaxation time for the mean state, where we take $\gamma = 100$; and T_R is the relaxation temperature that is described in sections 3a–c. The fast relaxation for the zonally mean state is chosen to allow reproduction of any chosen target profiles with a good accuracy, such that the zonal- and time-mean temperature in a simulation is approximately the relaxation temperature. This allows us to systematically change different aspects of the temperature field (e.g., the meridional temperature gradient and the vertical temperature gradient) in different regions of the atmosphere and investigate how these changes affect the eddy fields.

There are different methods to control the mean temperature field (e.g., Lunkeit et al. 1998; Chang 2005; Yuval and Kaspi 2016), and in appendix B it is demonstrated that the method we used in Yuval and Kaspi (2016) gives similar results to the simulations in this paper, indicating the results are invariant to the method used to control the temperature field. Interestingly, the heating formulation used here and the heating formulation that was used in Yuval and Kaspi (2016), which has a more realistic relaxation time, produce similar magnitude of eddies (appendix B). In the heating formulation used here, the zonal-mean temperature field at every time instance is very similar to the time- and zonal-mean temperature field, while in Yuval and Kaspi (2016), the zonal mean at every time instance will not necessarily be similar to the time mean, and therefore the temperature field is less constrained and fluctuates more. A possible drawback of the strong relaxation of the zonal temperature used in this study is that it might interfere with eddy life cycle at the stage eddies act to change the mean fields, and consequently eddies would have different magnitudes owing to the strong zonal-mean relaxation. However, since the eddies are similar in the two cases, it implies that the deviations of the zonal mean at every time instance from its time mean in the case of realistic relaxation time, does not contribute significantly to eddy amplitudes.

3. Temperature profiles in the simulations

To study how the vertical structure of baroclinicity changes the relation between MAPE, EKE, and eddy fluxes, the meridional and vertical temperature gradient are modified systematically. The temperature modifications simulated are of three types:

- Changes in the meridional temperature gradient at different levels of the troposphere (see section 3a). These temperature changes also induce changes in the lapse rate.
- Changes in the vertical temperature gradient (i.e., lapse rate) at different levels of the troposphere, while keeping the meridional temperature gradient constant (see section 3b).
- Changes in the meridional temperature gradient at different latitudes within the baroclinic region, while keeping the lapse rate unchanged (see section 3c).

Throughout this paper, the reference temperature T_{ref} is the equilibrium temperature structure of a simulation performed using Held and Suarez (1994) forcing including a dry convection scheme that relaxes the atmosphere to a lapse rate of $0.7\Gamma_{\mathrm{dry}}$, where $\Gamma_{\mathrm{dry}} = g/c_p$ is the dry adiabatic lapse rate. The dry convection scheme relaxes the temperature lapse rate to the value of $0.7\Gamma_{\mathrm{dry}}$

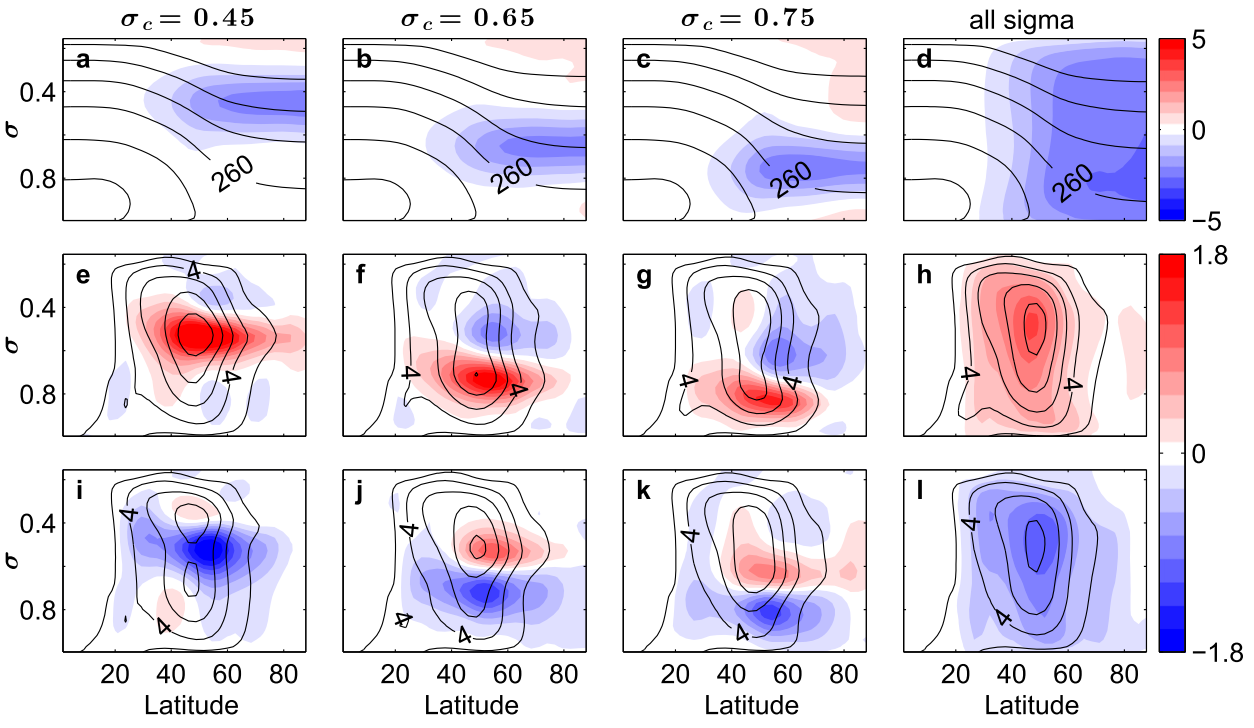

FIG. 1. (a)–(d) The temperature and (e)–(l) the Eady growth rate ($\times 10^6$) for simulations where the temperature gradient was (a)–(h) increased or (i)–(l) decreased by 10% in the (a),(e),(i) upper, (b),(f),(j) mid-, (c),(g),(k) lower troposphere and (d),(h),(l) in all levels of the atmosphere. Contours show the temperature and the Eady growth rate, and colors show the deviation from the reference simulation. The contour intervals are 15 K for temperature and 2 s^{-1} for Eady growth rate.

on a short time scale of 4 h when the lapse rate exceeds this value. The reference temperature profile is obtained using a simulation with a convection scheme in order to enable changing the lapse rate without creating statically unstable sections of the atmosphere. There is no convection scheme in any other simulation in this study.

a. *Changes in the vertical structure—Changes in meridional gradient and lapse rate*

Following Yuval and Kaspi (2016), the meridional temperature gradient of the reference run ($\partial_y T_{\mathrm{ref}}$) was modified only outside of the tropical region (poleward of latitude 24°), in the following manner:

$$T_R(|\phi|>24,\sigma) = T_{\mathrm{ref}}(\phi,\sigma) + x[T_{\mathrm{ref}}(\phi,\sigma) - T_{\mathrm{ref}}(|\phi|=24,\sigma)]\exp\left[-\frac{(\sigma-\sigma_c)^2}{2\delta\sigma^2}\right], \quad (2)$$

where σ is the vertical coordinate, T_R is the relaxation temperature and is also the target temperature field that the simulation obtains, x determines the fractional change in magnitude of the meridional gradient, σ_c is the vertical level where the maximal meridional temperature gradient is changed, $\delta\sigma$ determines the vertical interval of the temperature change, and $T_{\mathrm{ref}}(|\phi|=24,\sigma)$ is the reference temperature at latitude 24°.[1] The target temperature profiles are similar to those used in Yuval and Kaspi (2016) but a broader range of parameters is used here, which allows for an investigation of the relationship between MAPE and eddies when the vertical structure of baroclinicity is modified. Furthermore, Yuval and Kaspi (2016) used a different method to control the mean temperature, and in appendix B it is shown that the results of the two methods for these simulations are very similar.

The parameters used in the simulations are $x = 0$, ± 0.05, ± 0.10, ± 0.15, ± 0.20, ± 0.25 for $\sigma_c = 0.45, 0.65, 0.75, 0.85$ and $\delta\sigma = 0.1$ and $\delta\sigma \to \infty$ (when $\delta\sigma \to \infty$ the temperature gradient modifications are in all atmospheric levels). In Figs. 1a–d the temperature changes are presented in color for simulations where the temperature gradient was increased by 10% in the upper, mid-, and lower troposphere (Figs. 1a–c) and when the temperature gradient was modified in all atmospheric levels (Fig. 1d). Results are presented relative to the reference.

[1] Since the focus of this paper is the extratropical circulation, to minimize changes in the tropical circulation, the temperature field was kept constant equatorward of 24° latitude.

Since the meridional temperature gradient is modified by an amount that is proportional to the reference over the target region, regions with larger temperature gradient will be modified more, and this might play a role in the results. It was verified with another set of simulations (not shown) that the results of this study remain qualitatively the same also when the absolute value of the meridional temperature gradient is modified poleward of $\phi = 24°$.

b. *Changes in the vertical structure—Changes in the lapse rate*

The temperature profile was modified such that the lapse rate was changed in chosen vertical levels in the following manner:

$$T_R = \begin{cases} T_{\mathrm{ref}}(\phi,\sigma) & @ \quad \sigma > \sigma_1 \\ T_{\mathrm{ref}}(\phi,\sigma) - A[z(\sigma) - z(\sigma_1)] & @ \quad \sigma_1 > \sigma > \sigma_2 \\ T_{\mathrm{ref}}(\phi,\sigma) - A[z(\sigma_2) - z(\sigma_1)] & @ \quad \sigma < \sigma_2 , \end{cases}$$

where $z(\sigma)$ is the averaged geopotential height of a σ surface and A is the change in the lapse rate between the levels σ_1 and σ_2. The parameters used in this study are $A = \pm 0.5, \pm 1, \pm 1.5, \pm 2\,\mathrm{K\,km^{-1}}$ for $(\sigma_1, \sigma_2) = [(0.45, 0.25), (0.55, 0.35), (0.65, 0.45), (0.75, 0.55), (0.85, 0.65), (0.95, 0.75), (0.99, 0.25)]$.[2] In Figs. 2a–c the changes in the temperature profiles (color) are plotted for cases where the lapse rate was modified in upper-, mid-, and lower-tropospheric levels. These temperature profile changes modify only the lapse rate and the mean temperature but not the meridional temperature gradient. The changes in the mean profile occur above the level of σ_1.

To verify that changes in the mean temperature in upper levels of the simulations do not lead to qualitative changes in the results, temperature profiles where the mean temperature in the upper troposphere was constant and only the levels below σ_2 were modified were used, namely

$$T_R = \begin{cases} T_{\mathrm{ref}}(\phi,\sigma) + A[z(\sigma_2) - z(\sigma_1)] & @ \quad \sigma > \sigma_1 \\ T_{\mathrm{ref}}(\phi,\sigma) - A[z(\sigma) - z(\sigma_2)] & @ \quad \sigma_1 > \sigma > \sigma_2 \\ T_{\mathrm{ref}}(\phi,\sigma) & @ \quad \sigma < \sigma_2 . \end{cases}$$

Since the modification in the mean temperature did not change the qualitative results of this study, these results are not shown.

[2] For $(\sigma_1, \sigma_2) = (0.99, 0.25)$ the simulations where $A = 1.5, 2\,\mathrm{K\,km^{-1}}$ are not plotted since the change in the MAPE for these simulations is much larger than for the rest of the simulations, though the qualitative conclusions of this study apply also if these simulations are taken into consideration.

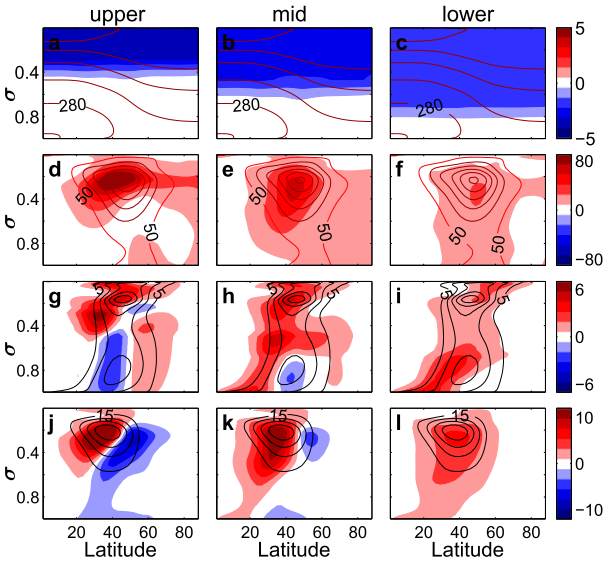

FIG. 2. (a)–(c) Temperature, (d)–(f) EKE, (g)–(i) EHF, and (j)–(l) EMF for simulations where the lapse rate was modified in the (left) upper $(0.25 < \sigma < 0.45)$, (center) mid- $(0.45 < \sigma < 0.65)$, and (right) lower $(0.65 < \sigma < 0.85)$ troposphere by $1\,\mathrm{K\,km^{-1}}$. Contours show the reference run values and the colors represents deviation from the reference. The contour intervals are 20 K for temperature, $50\,\mathrm{m^2\,s^{-2}}$ for EKE, $5\,\mathrm{m\,K\,s^{-1}}$ for EHF, and $15\,\mathrm{m^2\,s^{-2}}$ for EMF.

c. *Changes in the meridional structure—Changes in the meridional temperature gradient alone*

To isolate the effect on eddies of changes in the meridional temperature gradient from the changes in the lapse rate, the temperature gradient at different latitudes in the baroclinic zone was modified in the following manner:

$$T_R = \begin{cases} T_{\mathrm{ref}}(\phi,\sigma) & @ \quad \phi < \phi_1 \\ T_{\mathrm{ref}}(\phi,\sigma) - B(\phi - \phi_1) & @ \quad \phi_1 < \phi < \phi_2 \\ T_{\mathrm{ref}}(\phi,\sigma) - B(\phi_2 - \phi_1) & @ \quad \phi > \phi_2 , \end{cases}$$

where ϕ is latitude and B is the change in the meridional temperature gradient between latitudes ϕ_1 and ϕ_2. The parameters used in this study are $B = \pm 1/11, \pm 2/11\,\mathrm{K\,°^{-1}}$ and $(\phi_1, \phi_2) \approx [(29°, 40°), (35°, 46°), (38°, 49°), (40°, 51°), (43°, 54°), (46°, 57°), (48°, 59°), (51°, 62°)]$. The changes in the temperature profiles and zonal wind (color) are plotted Figs. 3a–d and 3e–h, respectively, for cases where the temperature gradient was modified equatorward of the center of the baroclinic zone (29°, 40°), in the center of the baroclinic zone (38°, 49°), poleward of the baroclinic zone center (46°, 57°), and significantly poleward of the baroclinic zone center (51°, 62°).

Unlike the temperature modifications in sections 3a and 3b, the vertical structure of the troposphere is not

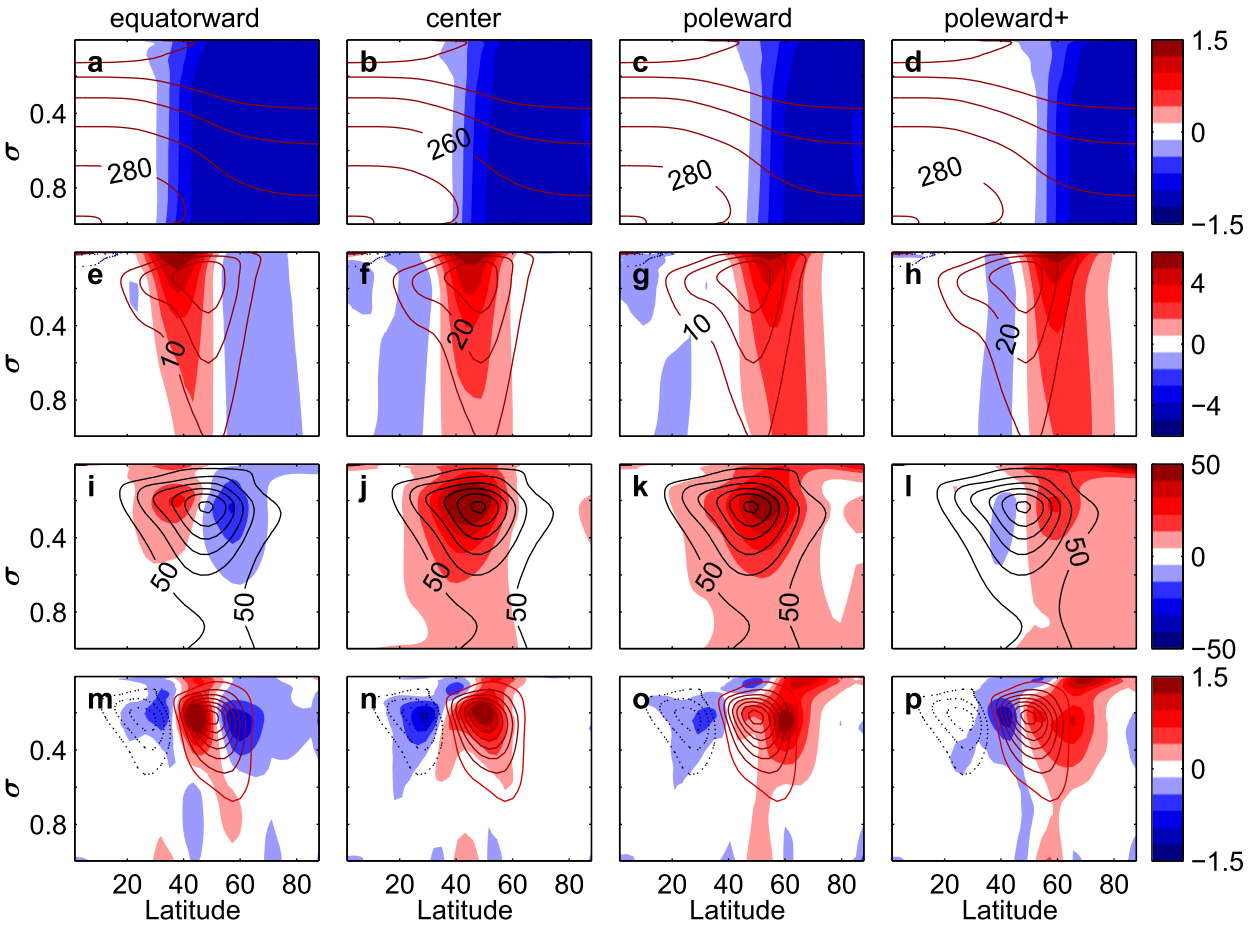

FIG. 3. (a)–(d) Temperature, (e)–(h) zonal wind, (i)–(l) EKE, and (m)–(p) EMF convergence ($\times 10^5$) for simulations where the meridional temperature gradient was modified (left)–(right) equatorward of the center of the baroclinic zone (29°, 40°), in the center of the baroclinic zone (38°, 49°), poleward of the baroclinic zone center (46°, 57°), and significantly poleward of the baroclinic zone center (51°, 62°) by $\pm 1/11\,\mathrm{K}^{\circ -1}$. Contours show the reference (dashed contours for negative values) run values and the colors represent deviation from the reference. The contour intervals are 20 K for temperature, $10\,\mathrm{m\,s^{-1}}$ for zonal wind, $50\,\mathrm{m^2\,s^{-2}}$ for EKE, and $1\,\mathrm{m\,s^{-2}}$ for EMF convergence.

modified when applying these temperature changes. These temperature changes modify the meridional structure of the temperature gradient without affecting the lapse rate. This allows for an investigation of how changes in the meridional temperature gradient structure affect eddies, and if the relation between EKE, eddy fluxes, and MAPE is sensitive to the meridional structure of the temperature gradient.

d. Calculation of MAPE

MAPE is calculated using the quadratic approximation of Lorenz (1955) in sigma coordinates. MAPE and integrated eddy quantities (EKE and eddy fluxes) are calculated in the baroclinic zone, which is defined as the region within 15° latitude of the maximum of the vertically integrated eddy heat flux, where the integral is performed from the level $\sigma_s = 0.95$, which is close to the surface, up to the tropopause $[\int_{\sigma_s}^{\sigma_t} \overline{v'\theta'}\cos(\phi)\,d\sigma]$.[3] The baroclinic zone, which is the region over which MAPE is calculated, will vary slightly between experiments as the latitude of maximum vertically integrated eddy heat flux varies. Choosing the baroclinic zone to be fixed between 26° and 65° or 30° and 60° does not qualitatively change the results. The resulting expression for the MAPE per unit area is

$$\mathrm{MAPE} = \int_{\sigma_t}^{\sigma_s} \frac{c_p p_0}{2g} \Gamma \left(\frac{\langle \overline{p} \rangle}{p_0}\right)^{\kappa} (\langle \overline{\theta}^2 \rangle - \langle \overline{\theta} \rangle^2)\, d\sigma, \qquad (3)$$

[3] The tropopause is defined as a level with zonal- and time-mean temperature lapse rate of $2\,\mathrm{K\,km^{-1}}$.

where $\langle A \rangle$ is the average over the baroclinic zone of field A, c_p is the heat capacity, g is the gravitational acceleration, σ_t is the tropopause height in the baroclinic region, θ is the potential temperature, $p_0 = 10^5$ Pa is a reference pressure, and $\Gamma = -(\kappa/\langle \overline{p} \rangle)\langle \partial \overline{\theta}/\partial p \rangle^{-1}$ is an inverse measure of static stability.

4. Results

The response of the eddy fields to changes in the vertical and meridional structure of baroclinicity is investigated, focusing mainly on the relation between MAPE, EKE, and eddy fluxes. Ideally, we would like to isolate the effects of changes in the vertical structure of the meridional and vertical temperature gradients on eddy fields. Modifying the vertical gradient (lapse rate) at chosen vertical levels without changing the meridional temperature gradient is possible, but changing the vertical structure of the meridional temperature gradient leads to changes in lapse rate, and it is not possible to isolate the changes in the vertical structure of the meridional temperature gradient. Therefore, the effects of changes in the meridional temperature gradient on eddy fields are investigated in two different manners. The results are divided into three sections: (i) changes in the vertical structure of baroclinicity (section 4a), where the meridional temperature gradient is changed at some atmospheric levels, and consequently also the vertical structure of the lapse rate is modified, but not the mean lapse rate; (ii) changes in the vertical structure of the lapse rate alone (section 4b); and (iii) changes in the meridional structure of the temperature gradient (section 4c), where the meridional temperature gradient is modified without modifying the lapse rate, but the vertical structure of baroclinicity is not modified. The last section also reveals how changes in the meridional temperature gradient at different latitudes lead to very different changes in the eddy fields.

Throughout this study, eddies are defined as the deviation from zonal and time mean, and eddy energies and fluxes are calculated using an integral over the baroclinic zone. The EHF and EMF contain a $\cos\phi$ factor (i.e., EHF $= \overline{v'\theta'\cos\phi}$ and EMF $= \overline{u'v'\cos\phi}$), where the prime denotes the deviation from the zonal and time mean.

a. *Modifying the baroclinicity at chosen vertical levels*

In Fig. 4 the EKE (Figs. 4a–c), EHF (Figs. 4d–f), and EMF (Figs. 4g–i) are plotted as a function of the temperature gradient percentage change, MAPE, and EAPE for simulations where the meridional temperature gradient was modified at different levels. Several interesting features are seen in the figure. 1) Figures 4a, 4d, and 4g show that eddies are more sensitive to changes in the meridional temperature gradient in the upper levels (blue dots) than in the mid- to lower troposphere (red, magenta, and orange dots). 2) Figure 4a shows that changing the temperature gradient in all vertical levels (gray dots) changes the EKE on the same order of magnitude as changing only the upper-tropospheric levels (blue dots). 3) Figure 4a shows that increasing (decreasing) the meridional temperature gradient in mid- to lower-tropospheric levels shown by the red and magenta dots causes a nonintuitive decrease (increase) in EKE, which is seen in Fig. 4b as a negative slope between EKE and MAPE. 4) Figure 4b shows that each color has an approximate linear relationship between MAPE and EKE, but with a different slope, implying no universal relationship between MAPE and EKE. For example, the blue and gray dashed lines are the best linear fit for the blue and gray dots, and the slopes of these lines have almost a factor-of-2 difference (1.86 and 1.01). 5) Figure 4c shows that the EKE and EAPE have an approximate linear relation. 6) Figures 4e and 4h show that eddy fluxes and MAPE have an approximate linear relation. 7) Figures 4f and 4i show that eddy fluxes and EAPE have noticeable deviations from linear scaling.

To understand the changes in the eddy fields, the changes in the local Eady growth rate [$\lambda = 0.31(g/NT)|\partial T/\partial y|$; Lindzen and Farrel 1980], which is used as a measure for baroclinicity, are plotted in Figs. 1e–l for cases where the temperature gradient was modified by ±10% (in Figs. 1e–h, $x = 0.1$; in Figs. 1i–l, $x = -0.1$). The Eady growth rate and the MAPE are affected by changes in both the static stability and the meridional temperature gradient. Increasing or decreasing the temperature gradient only in some levels of the troposphere (Figs. 1a–c) causes the static stability to increase in some regions and decrease in others. Therefore, the Eady growth rate can decrease (increase) in some regions even if the temperature gradient is increased (decreased); see Figs. 1e–g (decreased, Figs. 1i–k). Increasing (decreasing) the temperature gradient in all atmospheric levels leads to an increase (decrease) in the Eady growth rate at all levels of the atmosphere since the static stability is approximately unchanged while the temperature gradient increases (decreases) at all levels (Figs. 1h,l).

In the reference simulation, the baroclinicity is concentrated in the mid- to upper troposphere (see Figs. 1h,l for the Eady growth rate when the gradient is modified at all levels, and the vertical structure is nearly unmodified). When changing the temperature gradient in the upper troposphere, the baroclinicity is modified in

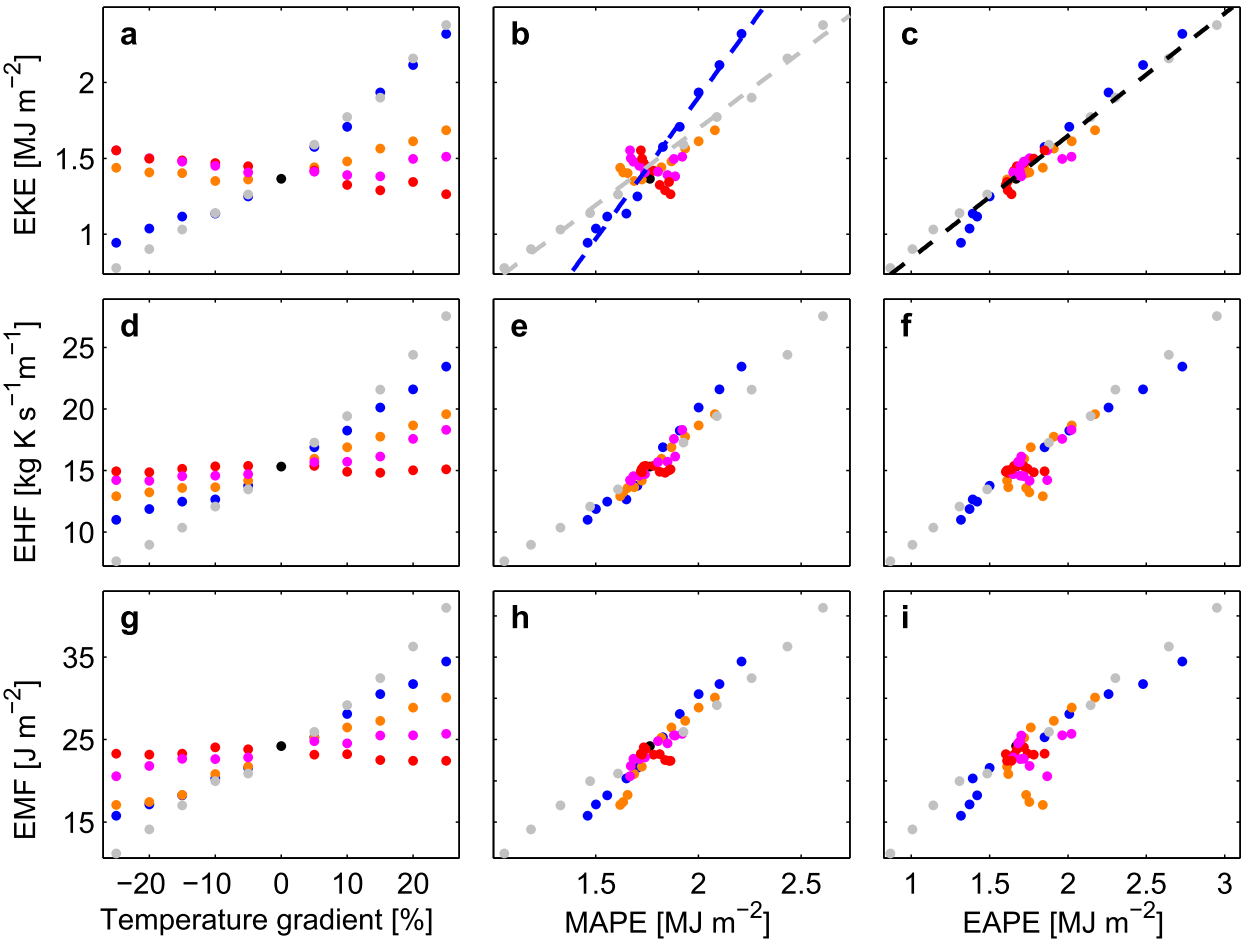

FIG. 4. (a)–(c) EKE, (d)–(f) EHF ($\times 10^{-4}$), and (g)–(i) EMF ($\times 10^{-4}$) as a function of the (left) meridional temperature gradient percentage change, (center) MAPE, and (right) EAPE. The colors show different vertical levels of meridional temperature gradient change for the upper level ($\sigma_c = 0.45$, blue), midlevel ($\sigma_c = 0.65$, orange), mid- to lower levels ($\sigma_c = 0.75$, magenta), lower levels ($\sigma_c = 0.85$, red), and all levels of the troposphere (gray). The gray and blue dashed lines in (b) are linear fits for the gray and blue dots and have slopes of 1.01 and 1.86, respectively. The black dashed line in (c) is a fit to all the points and has a slope of 0.80.

the region of maximal baroclinicity (Figs. 1e,i), which causes the largest change in the MAPE compared to other levels, and the response of the EKE and eddy fluxes is largest (blue dots in Fig. 4b).[4] When comparing two simulations with modified gradients, a larger MAPE change in one of the simulations does not necessarily mean a larger change in EKE of the simulation (e.g., compare the blue and gray dots in Fig. 4b). For example, in the simulation set considered in this section, the EKE is most sensitive to changes in MAPE when the upper-tropospheric temperature gradient is modified. We conclude that there is no linear scaling with a unique slope relating between MAPE and EKE even when all parameters in the simulations (except the relaxation temperature) are similar. In appendix C it is shown that the deviation from linear relation occurs also in the relation between EAPE and MAPE, implying that the closure suggested by Schneider and Walker (2008) is not robust for these simulations.

The decrease in EKE in response to an increase in the meridional temperature gradient in the mid- to lower levels is surprising, although a decrease in EKE when the meridional temperature gradient increases is seen also in observations of the northern Pacific winter (Nakamura 1992). Increasing the temperature gradient in the mid- or lower troposphere (Figs. 1b,c) leads to an increase in the Eady growth rate on average, but it increases in the mid- to lower levels where the reference baroclinicity is smaller and decreases at

[4] When increasing (decreasing) the temperature gradient, the largest increase (decrease) in baroclinicity happens below this level because of the changes in the static stability (Figs. 1e–l).

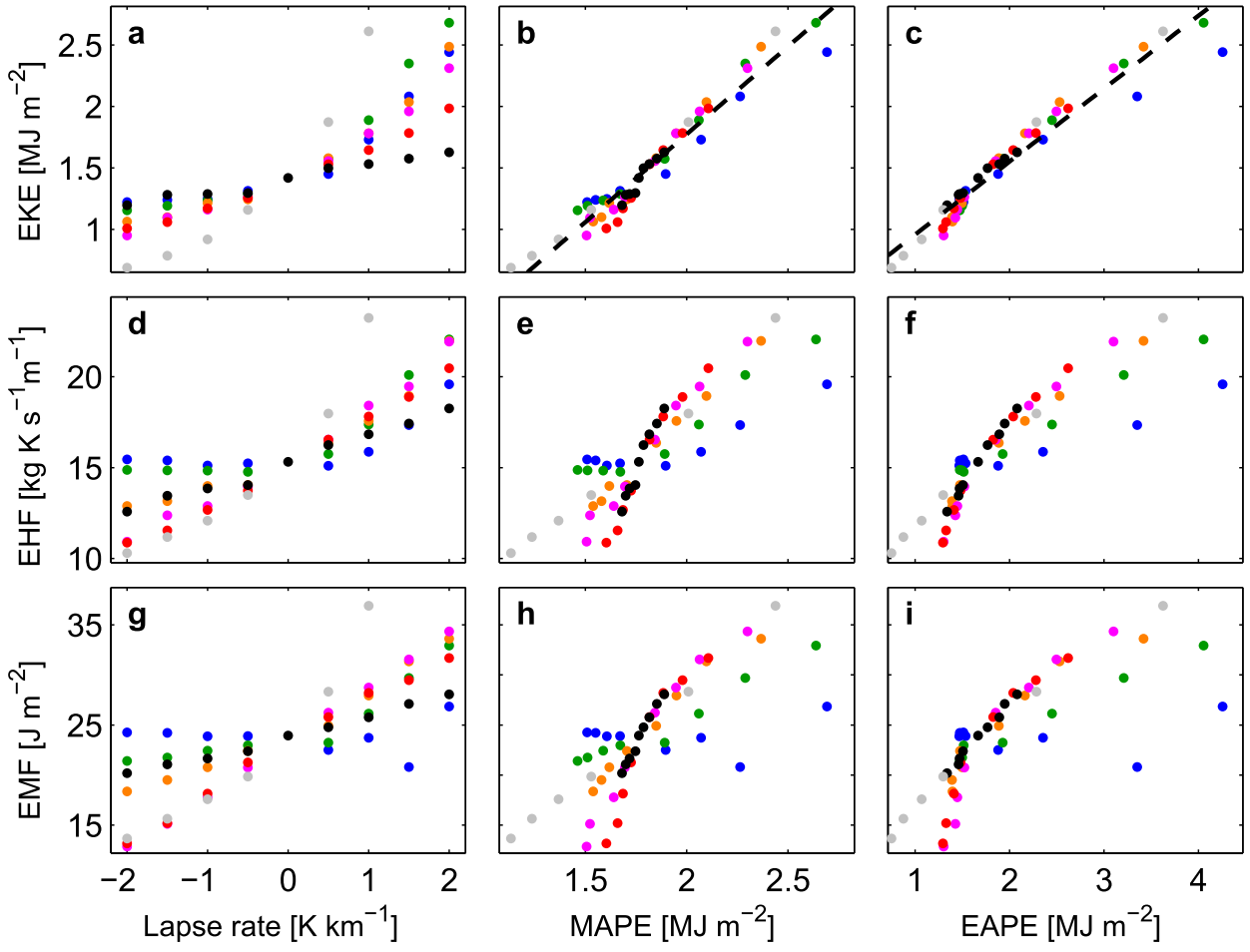

FIG. 5. (a)–(c) EKE, (d)–(f) EHF ($\times 10^{-4}$), and (g)–(i) EMF ($\times 10^{-4}$) as a function of the (left) lapse-rate change, (center) MAPE, and (right) EAPE for different simulations where the lapse rate was modified at different vertical levels. The colors show different vertical levels of lapse-rate change: in the upper level ($0.25 < \sigma < 0.45$, blue; $0.35 < \sigma < 0.55$, dark green), midlevel ($0.45 < \sigma < 0.65$; orange, $0.55 < \sigma < 0.75$, magenta), lower level ($0.65 < \sigma < 0.85$; red, $0.75 < \sigma < 0.95$, black), and throughout the troposphere ($0.25 < \sigma < 0.99$, gray). The black dashed line in (b) is the best linear fit for all the dots and has a slope of 1.42. The black dashed line in (c) is a fit to all the points and has a slope of 0.59.

higher levels where the reference baroclinicity is larger (Figs. 1e,f). On the other hand, decreasing the temperature gradient in the mid- to lower troposphere leads to a decrease in the mean baroclinicity, but the regions where it increases are of larger baroclinicity (Figs. 1j,k). Therefore, we hypothesize that the reason for the small increase in EKE when reducing the temperature gradient in the lower troposphere is the increased concentration of baroclinicity in the mid- to upper levels.

Interestingly, the vertically integrated EHF and EMF scale almost linearly with MAPE with the exception of modifying the gradient in lower levels (red dots, Figs. 4e,h). As shown in the next section, when changing the vertical structure of the lapse rate, the MAPE and eddy fluxes do not have linear relation.

b. Modifying the lapse rate at chosen vertical levels

In many studies that relate eddy fields to mean fields, the vertical structure of the lapse rate is not taken into account, and only the vertically averaged lapse rate is taken (e.g., Stone 1972; Held 1978). This is typically done because it enables one to deduce simple scaling relations. To understand to what extent the vertical structure of the lapse rate plays a role in affecting eddies and whether using the vertically mean lapse rate is sufficient when deriving scaling relations between eddies and mean quantities, the lapse rate was modified at different vertical levels separately.

In Fig. 5 the EKE (Figs. 5a–c), EHF (Figs. 5d–f), and EMF (Figs. 5g–i) are plotted as a function of the lapse-rate amplitude change, MAPE, and EAPE for

simulations where the lapse rate was modified at different vertical levels as described in section 3b. The main results are as follows. 1) Changing the lapse rate with a certain amplitude at different vertical levels results in very different amplitude changes in EKE and eddy fluxes (Figs. 5a,d,g). This implies that the vertical structure of the lapse rate plays an important role in determining eddies' amplitude, and knowledge regarding the mean lapse rate is not sufficient in order to determine eddy amplitudes. 2) Figure 5 shows that changing the lapse in all tropospheric levels induces the largest change in eddy quantities. This is expected, but underlined here since when the meridional temperature gradient is changed in all vertical levels, the change in eddies was not larger than when only the upper levels where modified (Fig. 4). 3) Increasing the lapse rate induces larger changes in the EKE than decreasing it (Fig. 5a).[5] 4) Changes in the upper-tropospheric lapse rate that lead to a large increase in EKE (Fig. 5a) do not increase significantly eddy fluxes (Figs. 5d,g, blue dots). 5) EKE and MAPE (Fig. 5b) as well as EKE and EAPE (Fig. 5c) have an approximate linear relation for these simulations. 6) MAPE and eddy fluxes do not have a linear relation in these simulations, and changes in the lower-level lapse rate lead to a larger sensitivity in eddy fluxes to MAPE changes (see black dots' slope in Figs. 5e,h).

To explain why the EKE response is not symmetric when the lapse rate is modified, one can consider the fact that $\mathrm{MAPE} \propto N^{-1}$. Combining this with the approximate linear relation between the MAPE and the EKE shown in Fig. 5b results in the lapse-rate increase inducing a larger EKE response than when decreasing it.

The relation between EKE and MAPE is approximately linear for all simulations in this section, regardless of the level that the lapse rate is modified at (see dashed line in Fig. 5b). When considering all simulations, the relation between eddy fluxes and MAPE is not linear, but when considering each color separately, there is an approximate linear relation between eddy fluxes and MAPE, where each color has a different slope relating eddy fluxes and MAPE.[6] As the lapse rate is modified in the upper region of the troposphere, the slope that approximately relates MAPE to eddy fluxes is smaller. This is most pronounced when the lapse rate is modified in the upper part of the troposphere (blue and dark green dots in Figs. 5e and 5h), where at certain simulations, eddy fluxes even reduce, though the MAPE has increased. The opposite response of EKE and eddy fluxes was also shown to be present in the ocean (Ferrari and Nikurashin 2010).

To understand why the mean EHF and EMF have a weak response to changes in the lapse rate in the upper troposphere, the zonal-mean EKE, EHF, and EMF are plotted in Fig. 2 for simulations where the lapse rate was modified by $1\,\mathrm{K\,km^{-1}}$ in the lower, mid-, and upper troposphere. When the lapse rate is modified at the mid- to upper levels, the eddy fluxes have a mixed response (weaken in some regions and strengthen in others; Figs. 2g,h,j,k). For example, when the lapse rate is modified at chosen sigma levels, EHF tends to increase at these levels and above them, while below these levels, it tends to decrease or to have a mixed response. Therefore, the integrated response of the EHF and EMF is relatively weak when the lapse rate is modified in the upper levels of the troposphere.

c. *Changes in the meridional structure of the temperature gradient*

In section 4a the vertical structure of the meridional temperature gradient was modified, and consequently also the lapse rate was modified. In this section only changes in the meridional temperature gradient at different latitudes are induced, but the vertical structure is not modified and the lapse rate remains unchanged. These changes allow investigation into how the meridional structure of the meridional temperature gradient alone affects eddies. In Fig. 6 the EKE (Figs. 6a–c), EHF (Figs. 6d–f), and EMF (Figs. 6g–i) are plotted as a function of the meridional gradient change, MAPE, and EAPE for the simulations described in section 3c. The center of the baroclinic zone is defined here to be the maximal vertically integrated EHF and is found at 43° latitude in the reference simulation (and in most of the other simulations as well). It is found that EKE and eddy fluxes are more sensitive to changes in the meridional temperature gradient in the vicinity and slightly poleward of this latitude. Namely, the change in EKE and eddy fluxes is relatively small (and can even be negative) when the temperature gradient is concentrated equatorward of this region (blue dots) or if the change in the gradient is significantly poleward of this region (gray dots).

The simulations in this study are in a mixed subtropical-eddy driven jet regime, where the EMF convergence is negative a few degrees equatorward of the jet maximum decelerating it and positive at the jet peak and at the poleward flank of the jet accelerating it (see Fig. 3). One possible explanation for the weak eddy response to increased temperature gradient at the equatorward flank of the jet is that the shear is

[5] Also eddy fluxes are more sensitive to increase in the lapse rate than its decrease in most cases (Figs. 5d,f).

[6] Schneider and Walker (2008) showed that the surface eddy heat flux ($\overline{v_s'\theta_s'}$) scales linearly with MAPE [see Eq. (9) in Schneider and Walker (2008)]. Also plotting the surface EHF as a function of MAPE does not give a linear relation between the two.

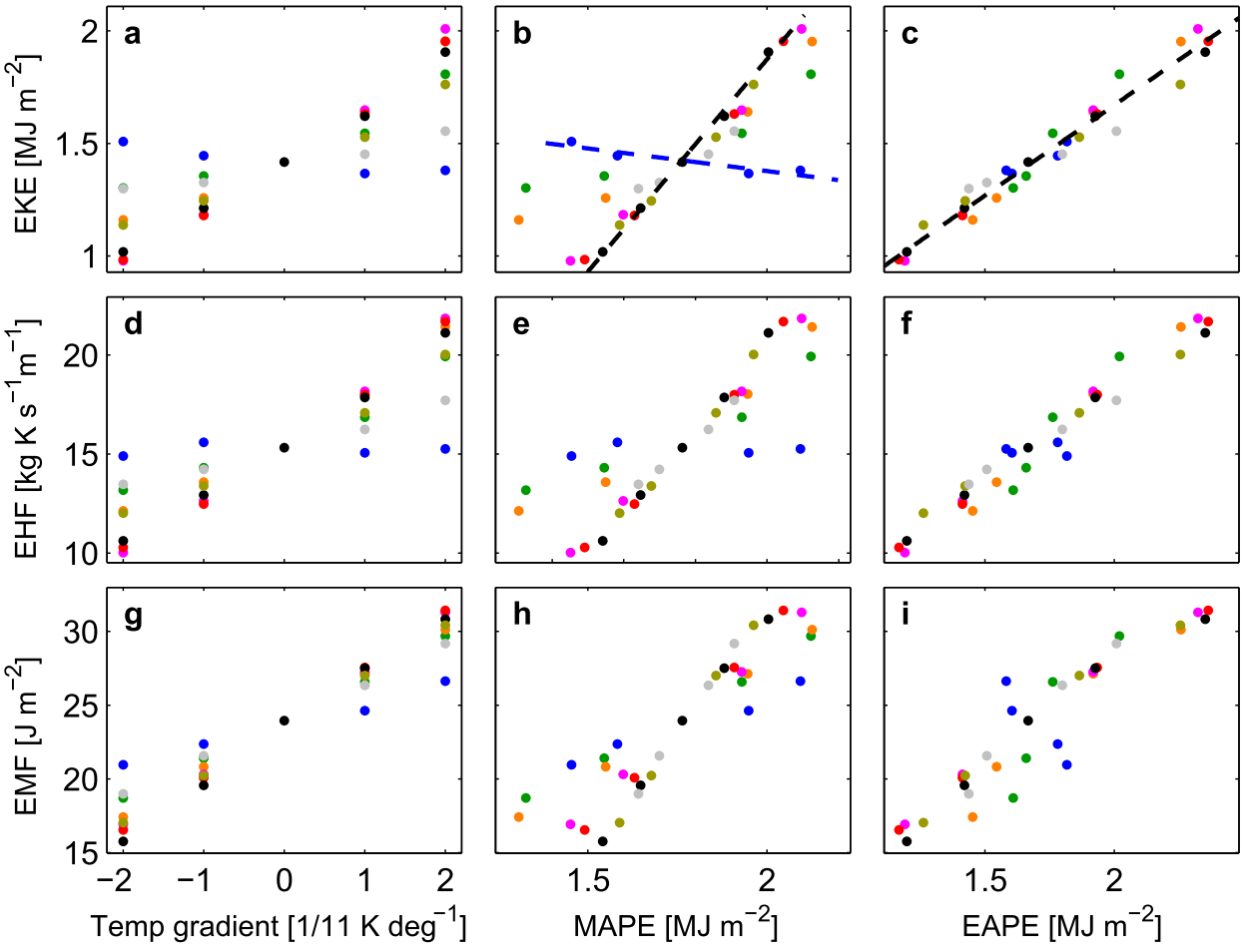

FIG. 6. (a)–(c) EKE, (d)–(f) EHF ($\times 10^{-4}$), and (g)–(i) EMF ($\times 10^{-4}$) as a function of the (left) meridional gradient change, (center) MAPE, and (right) EAPE for different simulations where the gradient was modified at different latitudes. The temperature gradient was modified between different latitudes [(29°, 40°), blue; (35°, 46°), dark green; (38°, 49°), orange; (40°, 51°), magenta; (43°, 54°), red; (46°, 57°), black; (48°, 59°), dark gray; and (51°, 62°), gray]. The black and blue dashed lines in (b) are the best linear fit for the black and blue dots and have a slope of 1.88 and −0.2. The black dashed line in (c) is a fit to all the points and has a slope of 0.80.

increased in regions where the jet is more subtropical and the EMF diverges and decelerates the jet (or has a mixed effect on the jet; Fig. 3m). On the other hand, when the temperature gradient is increased close to the jet peak or slightly poleward (Figs. 3f,g), where the jet is more eddy driven, the baroclinicity is increased where eddies accelerate the jet, and the increased baroclinicity tends to increase baroclinic eddies more (Figs. 3j,k,n,o). This explanation is consistent with the idea of Held et al. (2000) that is based on the concept that the Hadley cell edge (which is similar to the subtropical jet core) is at the point the atmosphere becomes baroclinically unstable. Therefore, when increasing the temperature gradient in the region of the subtropical jet, where the atmosphere is stable, the effect on eddies is minor. These results are consistent with previous studies that showed that stronger sea surface temperature (SST) gradients close to the jet center lead to a stronger eddy response than stronger SST gradients in regions that are significantly equatorward or poleward of this region (Brayshaw et al. 2008; Sampe et al. 2010) or other studies that showed that a strong subtropical jet is associated with a tendency to hamper eddies (Lachmy and Harnik 2014). When the temperature gradient is increased significantly poleward from the jet peak, the increase in EMF convergence is mostly poleward of the baroclinic zone and so is the (small) increase in EKE.

Figures 6b, 6e, and 6h show that eddies are less sensitive to changes in MAPE in regions where the gradient was changed in more equatorward regions (blue, green, and orange dots) and similar in other simulations. Furthermore, it is found that when the change in the gradient appears poleward of the baroclinic region center,

eddy fluxes, and EKE scale linearly with MAPE. As other simulations in this paper, in these simulations the EAPE and EKE have an approximate linear relation (Fig. 6c). These results show that the latitudinal region where the temperature gradient is modified plays an important role in determining eddy amplitudes, and this can have implications on how to define the baroclinic zone.

5. Summary and discussion

In this study, the eddy response and the relation between EKE and eddy fluxes to MAPE was investigated for cases where the meridional temperature gradient and the lapse rate were modified at different vertical and meridional sections of the atmosphere. Relating eddy quantities to the mean state is a fundamental topic in geophysical fluid dynamics, and it is found that the linear relationship between MAPE and eddies that was previously suggested becomes more complex when the vertical structure of baroclinicity is modified. The response of eddies to changes in the vertical structure of the meridional temperature gradient is extremely important in the context of global warming since future projections show that the equator-to-pole temperature gradient will decrease in the lower levels but will increase in the upper levels (e.g., Manabe and Wetherald 1975; Vallis et al. 2015).

To systematically simulate changes in the temperature field of the simulations, an idealized GCM was used with a Newtonian cooling scheme that relaxes the zonal-mean temperature with a short time scale to a chosen relaxation temperature, while the relaxation time for eddies was 100 times longer. This allowed for an accurate comparison of three types of temperature changes: (i) meridional temperature gradient changes at different vertical levels with changes in the lapse rate's vertical structure, (ii) lapse-rate changes at different vertical levels alone, and (iii) meridional temperature gradient changes at different latitudinal sections.

In addition to the relationship between MAPE and eddy fields, the sensitivity of eddies to the different temperature modifications was studied. We point out that this question is different from the relation between MAPE and eddy fields since similar amplitude changes in the temperature field at different sections of the atmosphere modify the MAPE differently, and therefore a large increase in eddies for a certain temperature change does not necessarily imply larger eddy sensitivity to MAPE changes. The main results of the study are as follows:

- MAPE is a nonlinear function of the meridional temperature gradient and of the lapse rate [MAPE $\approx (\partial_y T)^2/\partial_z T$], and therefore in regions where the meridional temperature gradient or lapse rate are large, a similar amplitude change in them will cause larger change in MAPE. Thus, if EKE and eddy fluxes scale linearly with MAPE it implies that eddies are more sensitive to meridional temperature gradient and lapse-rate changes where the baroclinicity is large.
- Using changes in MAPE as a first order approximation to EKE response to changes in the temperature field is qualitatively useful since there is a good correlation between changes in MAPE and EKE in most simulations (Figs. 4b, 5b, and 6b). On the other hand, the slope that relates between MAPE and EKE is not constant, implying that there is no universal relation between EKE and MAPE, and in some of the simulations shown in Figs. 4b and 6b there is even a negative slope relating EKE to MAPE (increase in MAPE can be accompanied by EKE decrease). Therefore, it is not quantitatively reliable to estimate EKE changes based on MAPE changes alone.
- It is found that when the vertical structure of the temperature gradient or lapse rate is modified, the largest response in EKE occurs when the baroclinicity is modified in regions where baroclinicity is predominantly large (Figs. 4a and 5a).
- In all simulations EKE and EAPE show an approximate linear relation, but different types of changes in the temperature field result in different slopes relating EAPE to EKE (see slopes of linear fits in Figs. 4c, 5c, and 6c).
- When the lapse rate is modified at different vertical levels, it is found that the EKE scales approximately linearly with MAPE (Fig. 5b). Since similar amplitude changes in the lapse rate at different levels of the troposphere cause very different MAPE changes, this result implies that the vertical structure of the lapse rate has a large effect on eddies. Therefore, the vertical mean lapse rate that is commonly used in theoretical considerations might not be an accurate measure for a troposphere with a lapse rate that changes significantly with altitude.
- When the meridional temperature gradient is modified at different latitudes in the baroclinic zone, it is found that eddies are less sensitive to changes at the equatorward regions of the baroclinic zone, which tends to strengthen the subtropical jet, and more sensitive to changes in the gradient at the center/poleward of the jet where momentum convergence drives the (eddy driven) jet (Figs. 6a,d,h). These results are consistent with previous studies that showed that eddies are more sensitive to an increase in the SST gradient at the center of the jet than at regions that are significantly poleward or equatorward of the jet center (Brayshaw et al. 2008; Sampe et al. 2010).

The baroclinic adjustment hypothesis (Stone 1978; Schneider 2004) suggests that baroclinic eddies maintain the extratropical troposphere neutral with respect to linear baroclinic instability when averaging on the extratropical troposphere. A possible interpretation of the increased eddy activity as a result of increased baroclinicity concentration is that when there is a local concentration of baroclinicity, there is a region that stores a large amount of potential energy that is highly unstable, and in this region, stronger eddy fluxes are needed to maintain a neutral mean flow. This explanation is similar to the adjustment hypothesis but implies that the adjustment occurs on smaller scales.

Acknowledgments. We thank the three reviewers for their very constructive comments that helped to improve the quality of this work. This research has been supported by the Israel Science Foundation (Grant 1819/16).

APPENDIX A

Sensitivity of the Linear Growth Rate to the Vertical Structure of Wind Shear

Held and O'Brien (1992) used a three-layer QG model with the β-plane approximation to study how eddies respond to changes in the vertical structure of the wind shear. Using linear instability analysis, they showed that for wind shear that is concentrated in the lower layer of their model the growth rate is larger than when it is concentrated in the upper layer for the same mean shear. On the other hand, in Yuval and Kaspi (2016) we showed that the maximal growth rate for an Eady-like model with stepwise shear is mostly sensitive to shear concentration and demonstrated that when the shear is predominantly concentrated in the upper level the growth rate is more sensitive to changes in the upper-level shear.

Here it is demonstrated in a simple 1D Eady-like model that the results of Held and O'Brien (1992) and Yuval and Kaspi (2016) can coexist. The inviscid QG potential vorticity (PV) equation, linearized about the local mean state characterized by the zonal mean $U = U(z)$ is used with a constant static stability N^2. The mean PV gradient can be written as $\partial_y Q = \beta - \partial_z[(f^2/N^2)U_z]$ with $\beta = 2\Omega R\cos(\theta)$, where R is the radius, Ω is the rotation rate, and subscripts denote derivatives. To solve the linear growth rate for different mean states, the method introduced by Smith (2007) is used, and details of the numerical scheme can be found there. All of the mean states used depend only on the vertical coordinate, and the obtained growth rates are for a 1D problem.

To take into account shear profiles that are concentrated in the upper and lower regions of the troposphere, the following wind profiles are considered:

$$U_{\text{up}} = U_{\text{top}}\frac{z^n}{H^n} \tag{A1}$$

and

$$U_{\text{low}} = U_{\text{top}} - U_{\text{top}}\frac{(H-z)^n}{H^n}, \tag{A2}$$

where H is the upper level of the model, which is taken it to be $H = 10\,\text{km}$; $U_{\text{top}} = 10\,\text{m s}^{-1}$ is the wind at the upper level; U_{up} is the case that the shear is concentrated in the upper atmosphere; and U_{low} is the case the wind is concentrated in the lower atmosphere. The parameter n controls the shear concentration and is taken to be larger or equal to 1. The constant shear problem (Eady problem) is the case where $n = 1$.

Figures A1a and A1b show the growth rates and wind profiles for different choices of shear, with $\beta = 0$. It is evident that the growth rate is sensitive to the concentration of baroclinicity, but the growth rate is affected similarly for lower and upper concentrations. This result is qualitatively similar to the result obtained by Yuval and Kaspi (2016), where for an Eady-like model with two different shears and $\beta = 0$, the growth rate was increased when the shear was more concentrated, regardless of the layer where it was concentrated.

Figures A1c and A1d show the growth rates for shear profiles that are concentrated in the upper and lower levels, with $\beta = 10^{-11}\,\text{s}^{-1}\,\text{m}^{-1}$. The figure shows that for moderate shear concentration ($n \sim 1$), in the presence of the β effect, a larger shear concentration at the lower levels increases the maximal growth rate, while larger shear concentration in the upper levels decreases the maximal growth rate.[A1] This result is similar to the result introduced in Held and O'Brien (1992, Fig. 1 therein). For all the cases tested, it was found that for similar mean shear, an increase in the shear concentration in the lower levels leads to increase in the maximal growth rate.

On the other hand, the reduction in the growth rate as we concentrate the shear more and more in the upper level does not hold when the shear concentration becomes larger. Figures A1e and A1f show that when the shear is largely concentrated in the upper region, an increased shear in the upper levels tends to increase the growth rate. To see this, we take the red dotted line in

[A1] The existence of a region that an increased shear in the upper regions decreases the growth rate depends on the exact parameters used in the model—see also Fig. A2.

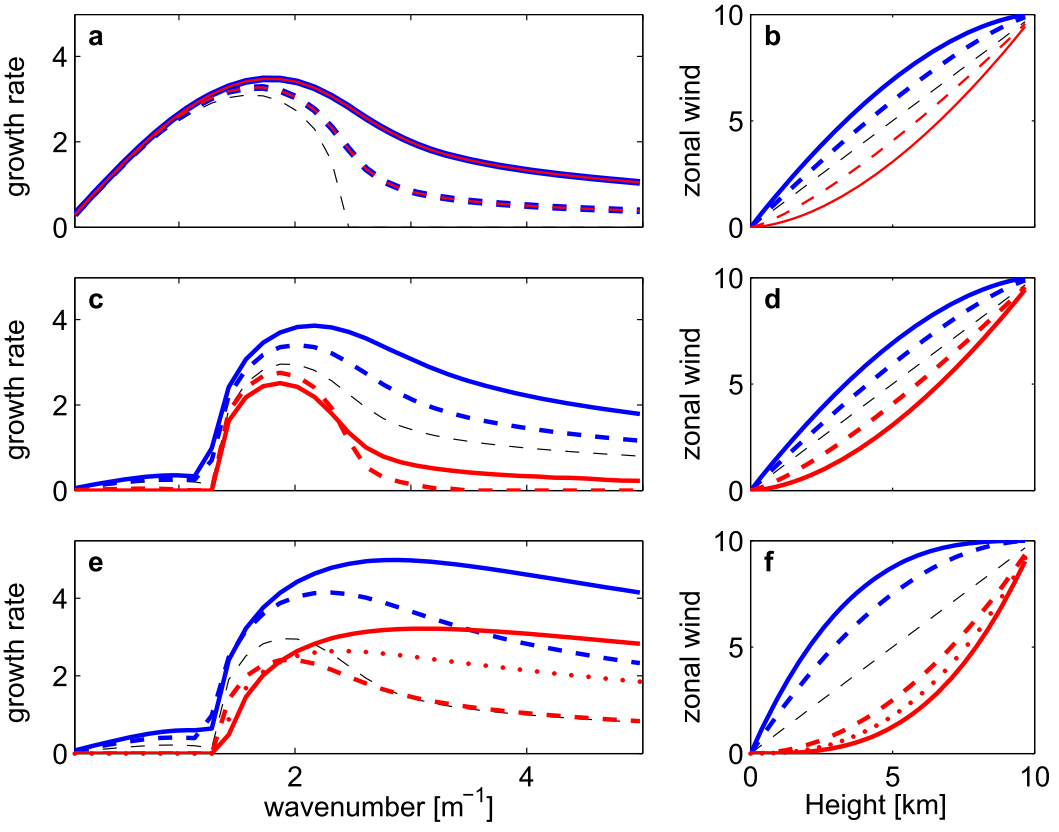

FIG. A1. (a),(c),(e) The growth rate as a function of the zonal wavenumber for different choices of shear and β and (b),(d),(f) the wind profiles as a function of height. Linear shear is in black ($n = 1$), lower-level shear concentration is in blue, and upper-level shear concentration is in red. In (a) and (b) $n = 1.3$ (dashed), $n = 1.7$ (solid), and $\beta = 0$; in (c) and (d) $n = 1.3$ (dashed), $n = 1.7$ (solid), and $\beta = 10^{-11}$ s^{-1} m^{-1}; and in (e) and (f) $n = 2$ (dashed), $n = 2.5$ (dotted), $n = 3$ (solid), and $\beta = 10^{-11}$ s^{-1} m^{-1}.

Fig. A1e as the reference state ($n = 2.5$) and increase the upper shear to a state described by the solid red line ($n = 3$), which has a larger maximal growth rate (Figs. A1e,f). On the other hand, an increase in the lower-level shear concentration (described by the dashed red line, $n = 2$) has a smaller maximal growth rate than the dotted line. Finally, we conclude that for a state that has a large shear concentration in the upper levels, a further increase in the upper-level shear concentration (while keeping a constant mean shear, meaning a decrease in the lower-level shear) will increase the growth rate, while an increase in the lower-level shear concentration in the lower levels (accompanied with a decrease in the upper-level shear) will decrease the maximal growth rate.

To summarize the results, Fig. A2 shows the maximal growth rate as a function of the upper-level shear concentration [the power n in Eq. (A1)] and β for 30 different values of n and 11 different values of β. This figure demonstrates that in the presence of large enough β, the concentration of shear in the upper levels has a nonmonotonic relation with the growth rate. The values of β at Earth's extratropics ($\beta \approx 10^{-11}$ m^{-1} s^{-1} at latitude $\phi = 60°$) are in the regime where the growth rate is a nonmonotonic function of the shear concentration (Fig. A2), and this nonmonotonicity explains the discrepancy between the results of Held and Obrein (1992) and the results of Yuval and Kaspi (2016). For a constant height H, the ratio between the upper-level wind and β is the dominant factor that determines if the growth rate is a nonmonotonic function of the upper-level shear. The results shown here demonstrate that when the vertical mean shear is constant, upper-level shear concentration can decrease the maximal growth rate as obtained by Held and O'Brien (1992) in cases that the shear concentration is relatively small (Fig. A1c). On the other hand, in cases where the upper-level shear concentration is large and the mean vertical shear is constant, the maximal Eady growth rate increases when the upper-level shear is increased even more and decreases when lower-level shear is increased [similar to Yuval and Kaspi (2016)].

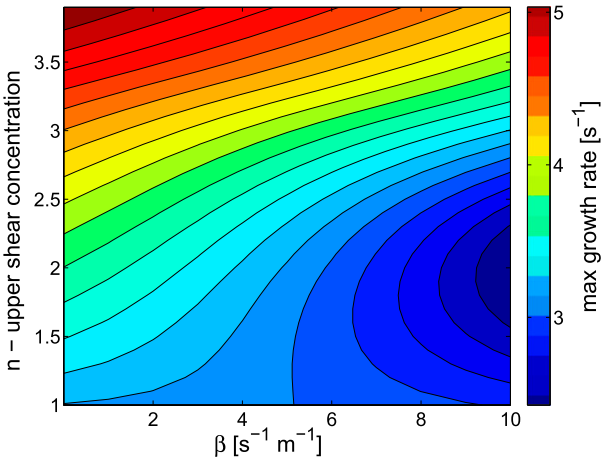

FIG. A2. The maximal growth rate ($\times 10^6$) as a function of β ($\times 10^{12}$) and the upper-level shear concentration n [see Eq. (A1)].

APPENDIX B

Consistency of Two Methods for Controlling the Mean Temperature

In this study a method that was suggested by Zurita-Gotor (2007) where the zonal-mean temperature and the deviations from the zonal-mean temperature (eddies) are relaxed with different relaxation times to a chosen profile was used. A very fast relaxation of the mean state was chosen, such that the mean temperature of the simulation is almost identical to the relaxation temperature. Lunkeit et al. (1998) and Yuval and Kaspi (2016) used a different method to control the mean state of the simulation by an iterative calculation of the relaxation temperature that will produce a chosen target temperature. In this method the relaxation time of the mean state and eddies is the same. Although the methods are different, it is shown here that for the case that the temperature gradient is modified at certain levels of the atmosphere, eddies respond similarly in both methods. This provides additional confidence that such methods enable prediction of a reliable response of eddy fields in response to changes in the mean temperature profile. In Fig. B1 the EKE, eddy momentum flux, and the eddy temperature flux are plotted for the case the temperature gradient was increased by 5% at different levels of the atmosphere using the method described in Yuval and Kaspi (2016), and in Fig. B2 the same quantities are plotted for the method used in this study (described in section 2b). The resemblance between Fig. B1 and Fig. B2 indicates that

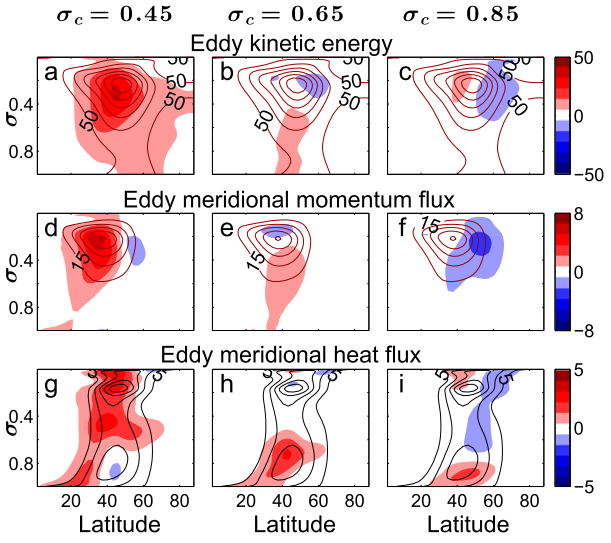

FIG. B1. (a)–(c) EKE, (d)–(f) EMF ($\overline{u'v'}$), and (g)–(i) EHF ($\overline{v'T'}$) for simulations where the meridional temperature gradient was modified at different levels with a gradient percentage change $x = 0.05$ using the method described in Yuval and Kaspi (2016). Colors show the deviation from the reference and contours represent reference simulation values. Contour intervals are 50 m^2 s^{-2} for EKE, 15 m^2 s^{-2} for EMF, and 5 K m s^{-1} for EHF.

the response of eddies to mean temperature changes are similar in the two methods.

It should be noted that the method used by Yuval and Kaspi (2016) also allows for obtaining zonal asymmetric mean temperature distribution [see also similar methods

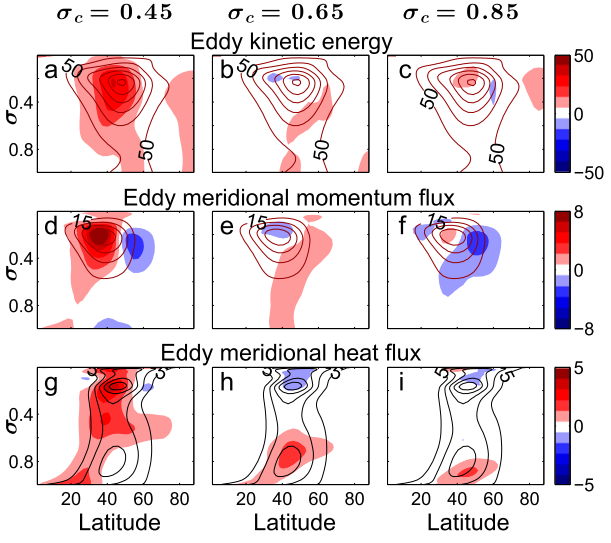

FIG. B2. (a)–(c) EKE, (d)–(f) EMF ($\overline{u'v'}$), and (g)–(i) EHF ($\overline{v'T'}$) for simulations where the meridional temperature gradient was modified at different levels with a gradient percentage change $x = 0.05$ using the method described in section 2b. Colors show the deviation from the reference and contours represent reference simulation values. Contour intervals are 50 m^2 s^{-2} for EKE, 15 m^2 s^{-2} for EMF, and 5 K m s^{-1} for EHF.

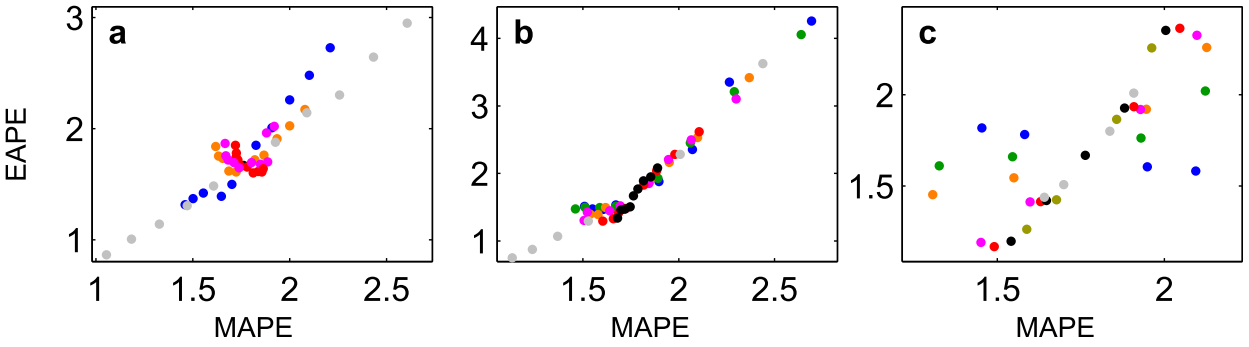

FIG. C1. EAPE as a function of MAPE for simulations where (a) the vertical structure of the meridional temperature gradient was modified (as in section 4a, colors as in Fig. 4), (b) the lapse rate was modified in different levels (as in section 4b, colors as in Fig. 5), and (c) when the meridional structure of the temperature gradient was modified (as in section 4c, colors as in Fig. 6).

with the asymmetric mean state in Lunkeit et al. (1998) and Chang (2005)], while the method described in section 2b was designed to obtain a zonal symmetric temperature distribution. The advantage in using the method used in this study is that it requires less computation time since the computation of the relaxation matrix is trivial (it is just the target temperature), while the method used by Yuval and Kaspi (2016) demands a separate simulation to obtain a relaxation matrix that produces the target temperature.

APPENDIX C

The Relation between EAPE and MAPE

To highlight that the deviations from linear scaling between eddy fields and the MAPE not only occur in the relation between EKE and MAPE, but also for the relation between the EAPE and MAPE, the EAPE and MAPE are plotted for different relaxation temperature profiles in Fig. C1. The figure shows that when the meridional and/or vertical structure of the meridional temperature gradient is modified, there are deviations from a linear relationship between EAPE and MAPE (Figs. C1a,c). When the lapse rate is modified, the relationship is close to linear (Fig. C1b), as is the relation between EKE to MAPE in these simulations (Fig. 5d). The relation between EAPE and MAPE in all the simulations in this paper qualitatively resemble the relation between the EKE and MAPE, such that the linear relation between EKE and EAPE still holds (Figs. 4g, 5g, and 6g).

REFERENCES

Brayshaw, D. J., B. Hoskins, and M. Blackburn, 2008: The storm-track response to idealized SST perturbations in an aqua-planet GCM. *J. Atmos. Sci.*, **65**, 2842–2860, doi:10.1175/2008JAS2657.1.

Chang, E. K. M., 2005: The impact of wave packets propagating across Asia on Pacific cyclone development. *Mon. Wea. Rev.*, **133**, 1998–2015, doi:10.1175/MWR2953.1.

Charney, J. G., 1947: The dynamics of long waves in a baroclinic westerly current. *J. Meteor.*, **4**, 136–162, doi:10.1175/1520-0469(1947)004<0136:TDOLWI>2.0.CO;2.

Eady, E. T., 1949: Long waves and cyclonic waves. *Tellus*, **1**, 33–52, doi:10.3402/tellusa.v1i3.8507.

Ferrari, R., and M. Nikurashin, 2010: Suppression of eddy diffusivity across jets in the Southern Ocean. *J. Phys. Oceanogr.*, **40**, 1501–1519, doi:10.1175/2010JPO4278.1.

Green, J. S. A., 1970: Transfer properties of the large-scale eddies and the general circulation of the atmosphere. *Quart. J. Roy. Meteor. Soc.*, **96**, 157–185, doi:10.1002/qj.49709640802.

Held, I. M., 1978: The vertical scale of an unstable baroclinic wave and its importance for eddy heat flux parameterizations. *J. Atmos. Sci.*, **35**, 572–576, doi:10.1175/1520-0469(1978)035<0572:TVSOAU>2.0.CO;2.

——, and E. O'Brien, 1992: Quasigeostrophic turbulence in a three-layer model: Effects of vertical structure in the mean shear. *J. Atmos. Sci.*, **49**, 1861–1870, doi:10.1175/1520-0469(1992)049<1861:QTIATL>2.0.CO;2.

——, and M. J. Suarez, 1994: A proposal for the intercomparison of the dynamical cores of atmospheric general circulation models. *Bull. Amer. Meteor. Soc.*, **75**, 1825–1830, doi:10.1175/1520-0477(1994)075<1825:APFTIO>2.0.CO;2.

——, and V. Larichev, 1996: A scaling theory for horizontally homogeneous, baroclinically unstable flow on a beta plane. *J. Atmos. Sci.*, **53**, 946–952, doi:10.1175/1520-0469(1996)053<0946:ASTFHH>2.0.CO;2.

——, and Coauthors, 2000: The general circulation of the atmosphere. *Proc. 2000 Program in Geophysical Fluid Dynamics*, Woods Hole, MA, Woods Hole Oceanographic Institute, 70 pp. [Available online at https://www.gfdl.noaa.gov/wp-content/uploads/files/user_files/ih/lectures/woods_hole.pdf.]

Hoskins, B. J., and P. J. Valdes, 1990: On the existence of storm-tracks. *J. Atmos. Sci.*, **47**, 1854–1864, doi:10.1175/1520-0469(1990)047<1854:OTEOST>2.0.CO;2.

Lachmy, O., and N. Harnik, 2014: The transition to a subtropical jet regime and its maintenance. *J. Atmos. Sci.*, **71**, 1389–1409, doi:10.1175/JAS-D-13-0125.1.

Li, C., and D. S. Battisti, 2008: Reduced Atlantic storminess during last glacial maximum: Evidence from a coupled climate model. *J. Climate*, **21**, 3561–3579, doi:10.1175/2007JCLI2166.1.

Lindzen, R. S., and B. Farrel, 1980: A simple approximate result for the maximum growth rate of baroclinic instabilities. *J. Atmos. Sci.*, **37**, 1648–1654, doi:10.1175/1520-0469(1980)037<1648:ASARFT>2.0.CO;2.

Lorenz, D. J., and D. L. Hartmann, 2001: Eddy–zonal flow feedback in the Southern Hemisphere. *J. Atmos. Sci.*, **58**, 3312–3327, doi:10.1175/1520-0469(2001)058<3312:EZFFIT>2.0.CO;2.

Lorenz, E. N., 1955: Available potential energy and the maintenance of the general circulation. *Tellus*, **7**, 157–167, doi:10.3402/tellusa.v7i2.8796.

Lunkeit, F., L. Fraedrich, and S. E. Bauer, 1998: Storm tracks in warmer climate: Sensitivity studies with a simplified global circulation model. *Climate Dyn.*, **14**, 813–826, doi:10.1007/s003820050257.

Manabe, S., and R. T. Wetherald, 1975: The effects of doubling the CO_2 concentration on the climate of a general circulation model. *J. Atmos. Sci.*, **32**, 3–15, doi:10.1175/1520-0469(1975)032<0003:TEODTC>2.0.CO;2.

Merlis, T. M., and T. Schneider, 2009: Scales of linear baroclinic instability and macroturbulence in dry atmospheres. *J. Atmos. Sci.*, **66**, 1821–1833, doi:10.1175/2008JAS2884.1.

Nakamura, H., 1992: Midwinter suppression of baroclinic wave activity in the Pacific. *J. Atmos. Sci.*, **49**, 1629–1642, doi:10.1175/1520-0469(1992)049<1629:MSOBWA>2.0.CO;2.

O'Gorman, P. A., 2010: Understanding the varied response of the extratropical storm tracks to climate change. *Proc. Natl. Acad. Sci. USA*, **107**, 19 176–19 180, doi:10.1073/pnas.1011547107.

——, and T. Schneider, 2008: Energy in midlatitude transient eddies in idealized simulations of changed climates. *J. Climate*, **21**, 5797–5806, doi:10.1175/2008JCLI2099.1.

Pavan, V., 1996: Sensitivity of a multi-layer quasi-geostrophic β-channel to the vertical structure of the equilibrium meridional temperature gradient. *Quart. J. Roy. Meteor. Soc.*, **122**, 55–72, doi:10.1002/qj.49712252904.

Sampe, T., H. Nakamura, A. Goto, and W. Ohfuchi, 2010: Significance of a midlatitude SST frontal zone in the formation of a storm track and an eddy-driven westerly jet. *J. Climate*, **23**, 1793–1814, doi:10.1175/2009JCLI3163.1.

Schneider, T., 2004: The tropopause and the thermal stratification in the extratropics of a dry atmosphere. *J. Atmos. Sci.*, **61**, 1317–1340, doi:10.1175/1520-0469(2004)061<1317:TTATTS>2.0.CO;2.

——, and C. C. Walker, 2008: Scaling laws and regime transitions of macroturbulence in dry atmospheres. *J. Atmos. Sci.*, **65**, 2153–2173, doi:10.1175/2007JAS2616.1.

Smith, K. S., 2007: The geography of linear baroclinic instability in Earth's oceans. *J. Mar. Res.*, **65**, 655–683, doi:10.1357/002224007783649484.

Stone, P. H., 1972: A simplified radiative-dynamical model for the static stability of rotating atmospheres. *J. Atmos. Sci.*, **29**, 405–418, doi:10.1175/1520-0469(1972)029<0405:ASRDMF>2.0.CO;2.

——, 1978: Baroclinic adjustment. *J. Atmos. Sci.*, **35**, 561–571, doi:10.1175/1520-0469(1978)035<0561:BA>2.0.CO;2.

Vallis, G. K., P. Zurita-Gotor, C. Cairns, J. Kidston, 2015: Response of the large-scale structure of the atmosphere to global warming. *Quart. J. Roy. Meteor. Soc.*, **141**, 1479–1501, doi:10.1002/qj.2456.

Wu, Y., M. Ting, R. Seager, H.-P. Huang, and M. A. Cane, 2011: Changes in storm tracks and energy transports in a warmer climate simulated by the GFDL CM2.1 model. *Climate Dyn.*, **37**, 53–72, doi:10.1007/s00382-010-0776-4.

——, R. Seager, M. Ting, N. Naik, and T. A. Shaw, 2012: Atmospheric circulation response to an instantaneous doubling of carbon dioxide. Part I: Model experiments and transient thermal response in the troposphere. *J. Climate*, **25**, 2862–2879, doi:10.1175/JCLI-D-11-00284.1.

Yuval, J., and Y. Kaspi, 2016: Eddy activity sensitivity to changes in the vertical structure of baroclinicity. *J. Atmos. Sci.*, **73**, 1709–1726, doi:10.1175/JAS-D-15-0128.1.

Zurita-Gotor, P., 2007: The relation between baroclinic adjustment and turbulent diffusion in the two-layer model. *J. Atmos. Sci.*, **64**, 1284–1300, doi:10.1175/JAS3886.1.